

γW -exchange contributions in neutron β decay in the forward-angle limit

Hui-Yun Cao^{1*}, Hai-Qing Zhou^{2†}

¹ School of Physics and Electronic Science, Hubei Normal University, HuangShi 435002, China

² School of Physics, Southeast University, NanJing 211189, China

(Dated: March 18, 2025)

In this work, the contributions from γW -exchange in neutron β decay are estimated at the amplitude level. Using a general form for the electromagnetic (EM) form factors (FFs) of the proton, the EM FFs of the neutron, and the weak FFs of the Wnp interaction as inputs, we present analytical expressions for the inner part of the γW -exchange amplitude under the forward angle limit. The differences and relations between our method and those used in the references are discussed. To compare our numerical results with those provided in the references, we consider three types of FFs as examples. The numerical results show that when the favored EM FFs are used, our result for the contribution from the Fermi part is consistent with those reported in the references, while our results for the Gamow-Teller parts are about 7% and 13% larger than those reported in Ref. [1].

I. INTRODUCTION

Neutron β decay is triggered by the electroweak interaction, where a free neutron decays into a proton, accompanied by the emission of an electron and an electron antineutrino ($n \rightarrow pe\bar{\nu}_e$). Due to its clean background, neutron β decay serves as a powerful laboratory for extracting the Cabibbo-Kobayashi-Maskawa (CKM) matrix V_{ud} in the Standard Model (SM) [2], which is important for checking the universality of the quark mixing [3]. Additionally, it can be used to extract the structure of the proton, such as the axial-vector coupling constant

* E-mail: caohy@hbnu.edu.cn

† E-mail: zhouhq@seu.edu.cn

g_A , which provides necessary input for nuclear physics, particle physics, astrophysics, and cosmology [4–6].

For neutron β decay, the value of V_{ud} is extracted from the experimental data via the following theoretical relation

$$|V_{ud}|^2 \propto \frac{1}{\tau_n(1+3\lambda^2)} \frac{1}{1+\text{RCs}}, \quad (1)$$

where τ_n is the neutron lifetime, $\lambda \equiv g_A/g_V$ with $g_{A,V}$ being the axial-vector and vector coupling constants of the Wnp interaction, and RCs denote the electroweak radiative corrections, which are related to the structures of the proton and neutron and should be calculated theoretically.

Protons and neutrons are bound by the strong interaction, and their structures are described by Quantum Chromodynamics (QCD). Due to the non-perturbative nature of QCD, it is still difficult to calculate RCs from first principles. For the RCs in free neutron β decay, as summarized in the literature [7], the best starting point is Sirlin’s representation. Sirlin [8] decomposes the RCs into outer (known as model-independent) and inner (known as model-dependent) parts as follows:

$$\text{RCs} = \frac{\alpha_e}{2\pi} \bar{g}(E_m) + \Delta_R^V, \quad (2)$$

where α_e is the fine structure constant, and the outer correction $\bar{g}(E_m)$ is a universal function that represents the extreme infrared part of the radiative correction and is exactly calculable. The inner correction Δ_R^V is related to short-range and hadronic structure effects, which are the main sources of uncertainty in extracting V_{ud} and λ from experimental data. The analyses in Refs. [9–11] give the inner RCs as

$$\Delta_R^V = \frac{\alpha_e}{2\pi} \left[3 \ln \frac{m_Z}{m_\rho} + \ln \frac{m_Z}{m_W} + \tilde{a}_g \right] + \delta_{\text{HD}}^{\text{QED}} + 2 \square_{\gamma W}^V, \quad (3)$$

where the first two terms on the right-hand side are the resummation of leading quantum electrodynamic (QED) logarithms, \tilde{a}_g is the perturbative QCD (pQCD) correction, and $\delta_{\text{HD}}^{\text{QED}}$ represents contributions from the leading logs of higher-order QED effects. The term $\square_{\gamma W}^V$ denotes the RCs originating from the γW -exchange diagrams, which can be expressed as

$$\square_{\gamma W}^V = \frac{\alpha_e}{2\pi} \left[\frac{1}{2} \ln \frac{m_W}{m_A} + C_{\text{Born}} + \frac{1}{2} \text{Ag} \right], \quad (4)$$

where the first term in the square brackets represents the large electroweak logarithm, with m_A as an effective IR cutoff scale, C_{Born} is the Born elastic contribution to the low-energy part of the γW -exchange diagram, and Ag is the pQCD correction.

Refs. [1, 12] calculated C_{Born} in the forward angle limit (FAL), where the proton and neutron are treated as isospin doublet states, and special combinations of their electromagnetic (EM) form factors (FFs) are used as inputs to estimate the contributions. In this study, we discuss the inner RCs of γW -exchange contributions to the amplitude of neutron β decay, and then relate these corrections to C_{Born} . In our calculation, we take the EM FFs of the proton and neutron as independent inputs since they are measured independently in different experiments. Furthermore, we use a very general form for these FFs as input to provide the analytic expressions for the γW -exchange amplitude. These analytical expressions can be used not only to estimate the corrections to the lifetime of the neutron, but also to estimate the corrections to all polarized measurements. Additionally, they can be utilized when the measurements of the EM FFs of the proton and neutron are improved in the future.

The paper is organized as follows. In Sec. II, we provide some basic formulas, including the expressions for the amplitudes, the approximations used in Refs. [1, 12], the existing problems, and the parameterization of the input FFs. In Sec. III, we express the amplitude as a combination of 16 terms in the form of Pauli spinors, and then present the analytical expressions for the coefficients of these 16 terms in the FAL. The relations between these coefficients and C_{Born} are also discussed. In Sec. IV, we take three types of FFs as inputs to present the numerical comparisons between our results and those reported in the literature. A detailed discussion of these numerical results and the conclusion are provided.

II. γW -EXCHANGE CONTRIBUTIONS

A. The One- W -exchange and γW -exchange amplitudes

At the hadronic level, the tree diagram for the neutron β decay can be described by Fig. 1, where only one- W -exchange diagram contributes. When considering the RCs from γW -exchange with the elastic intermediate state, the diagrams shown in Fig. 2 contribute,

and the corresponding amplitudes can be expressed as follows:

$$\begin{aligned}
\mathcal{M}^W &= -i \left[\bar{u}(p_e, m_e) \Gamma_{W\nu e}^\omega u(p_\nu, m_\nu) \right] \left[\bar{u}(p_p, m_p) \Gamma_{Wnp}^\mu(q) u(p_n, m_n) \right] \frac{-ig_{\mu\omega}}{q^2 - m_W^2}, \\
\mathcal{M}_{(a)}^{\gamma W} &= -i \int \frac{d^4k}{(2\pi)^4} \left[\bar{u}(p_e, m_e) \Gamma_{\gamma ee}^\beta S_F(p_e + k, m_e) \Gamma_{W\nu e}^\omega u(p_\nu, m_\nu) \right] \\
&\quad \times \left[\bar{u}(p_p, m_p) \Gamma_{\gamma pp}^\alpha(k) S_F(p_p - k, m_p) \Gamma_{Wnp}^\mu(q - k) u(p_n, m_n) \right] \frac{-ig_{\mu\omega}}{q^2 - m_W^2} \frac{-ig_{\alpha\beta}}{k^2 + i\epsilon}, \\
\mathcal{M}_{(b)}^{\gamma W} &= -i \int \frac{d^4k}{(2\pi)^4} \left[\bar{u}(p_e, m_e) \Gamma_{\gamma ee}^\beta S_F(p_e + k, m_e) \Gamma_{W\nu e}^\omega u(p_\nu, m_\nu) \right] \\
&\quad \times \left[\bar{u}(p_p, m_p) \Gamma_{Wnp}^\mu(q - k) S_F(p_n + k, m_n) \Gamma_{\gamma nn}^\alpha(k) u(p_n, m_n) \right] \frac{-ig_{\mu\omega}}{q^2 - m_W^2} \frac{-ig_{\alpha\beta}}{k^2 + i\epsilon}, \quad (5)
\end{aligned}$$

where $\bar{u}(p_e, m_e)$, $u(p_\nu, m_\nu)$, $\bar{u}(p_p, m_p)$ and $u(p_n, m_n)$ are the spinors of the electron, antineutrino, proton and neutron with the corresponding momentum and mass, respectively. Here $q \equiv p_p - p_n$ and k is momentum of photon. Additionally, the S_F is given by

$$S_F(l, m) = \frac{i(l+m)}{l^2 - m^2 + i\epsilon}, \quad (6)$$

and the vertices are

$$\Gamma_{\gamma ee}^\mu = -ie\gamma^\mu, \quad \Gamma_{W\nu e}^\mu = i\frac{g}{2\sqrt{2}}\gamma^\mu(1 - \gamma_5), \quad (7)$$

$$\Gamma_{\gamma pp}^\mu(l) = ie \left[F_1^p(l^2)\gamma^\mu + i\frac{F_2^p(l^2)}{2m_p}\sigma^{\mu\nu}l_\nu \right],$$

$$\Gamma_{\gamma nn}^\mu(l) = ie \left[F_1^n(l^2)\gamma^\mu + i\frac{F_2^n(l^2)}{2m_n}\sigma^{\mu\nu}l_\nu \right], \quad (8)$$

$$\Gamma_{Wnp}^\mu(l) = i\frac{g}{2\sqrt{2}}V_{ud} \left[\left(f_1(l^2)\gamma^\mu + i\frac{f_2(l^2)}{2m_N}\sigma^{\mu\rho}l_\rho + \frac{f_3(l^2)}{2m_N}l^\mu \right) \right] \quad (9)$$

$$+ \left(f_4(l^2)\gamma^\mu + i\frac{f_5(l^2)}{2m_N}\sigma^{\mu\rho}l_\rho + \frac{f_6(l^2)}{2m_N}l^\mu \right) \gamma_5 \Big], \quad (10)$$

where l is the momentum of the incoming photon or W boson, $e = -|e|$ is the EM interaction coupling constant, g is the $SU(2)$ gauge coupling constant, $m_N \equiv \frac{m_n + m_p}{2}$, $F_{1,2}^p(l^2)$ and $F_{1,2}^n(l^2)$ are the EM FFs of the proton and neutron, $f_1(l^2)$, $f_2(l^2)$, $f_3(l^2)$, $f_4(l^2)$, $f_5(l^2)$, and $f_6(l^2)$ account for vector, weak magnetism, scalar, axial vector, weak electricity, and induced pseudoscalar contributions, respectively.

In the above expressions, the on-shell FFs are used in the loop integration. One might question whether the nucleon could be off-shell in the loop diagrams, necessitating consideration of the off-shell effects. To address this, the dispersion relations (DRs) method or lattice

calculation is employed to estimate the corresponding contributions in Refs. [13–16]. It is important to note that the imaginary parts of the box diagrams are independent of off-shell effects, and the full results obtained from the above expressions automatically satisfy certain DRs, as indicated in the ep scattering case [17, 18]. This leads to a significant property: the differences between the real parts of the box diagrams calculated directly and those obtained using un-subtracted DRs are polynomial functions of momenta. These polynomials correspond to the subtracted terms in the DRs. In other words, both methods yield the same results when the same on-shell FFs are used as inputs, except for the presence of some polynomial terms. Furthermore, for finite q^2 , it is advisable to apply DRs at the amplitude level rather than at the cross-section level, as the latter approach may overlook contributions from kinematic singularities, such as the γZ -exchange contribution in ep scattering case [19].

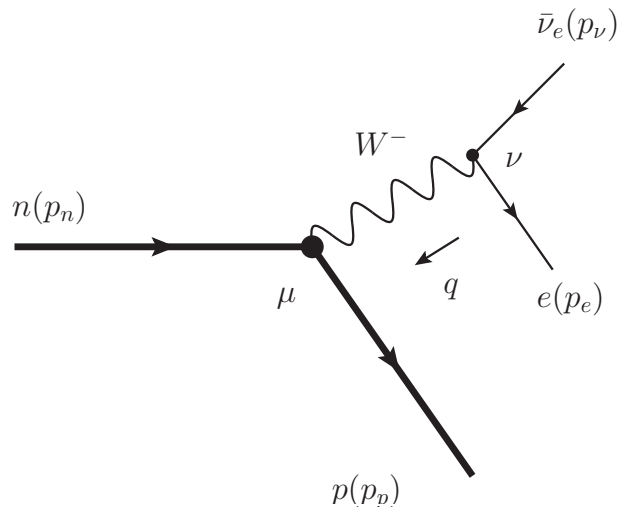


FIG. 1: Diagram for $n \rightarrow pe\bar{\nu}_e$ with one-W-exchange.

In the literature, the RCs are usually separated into inner contributions and outer contributions. For the former, it is equivalent to keeping only the terms with Levi-Civita tensors in the amplitude of the leptonic part after the products of Dirac matrices are reduced. This

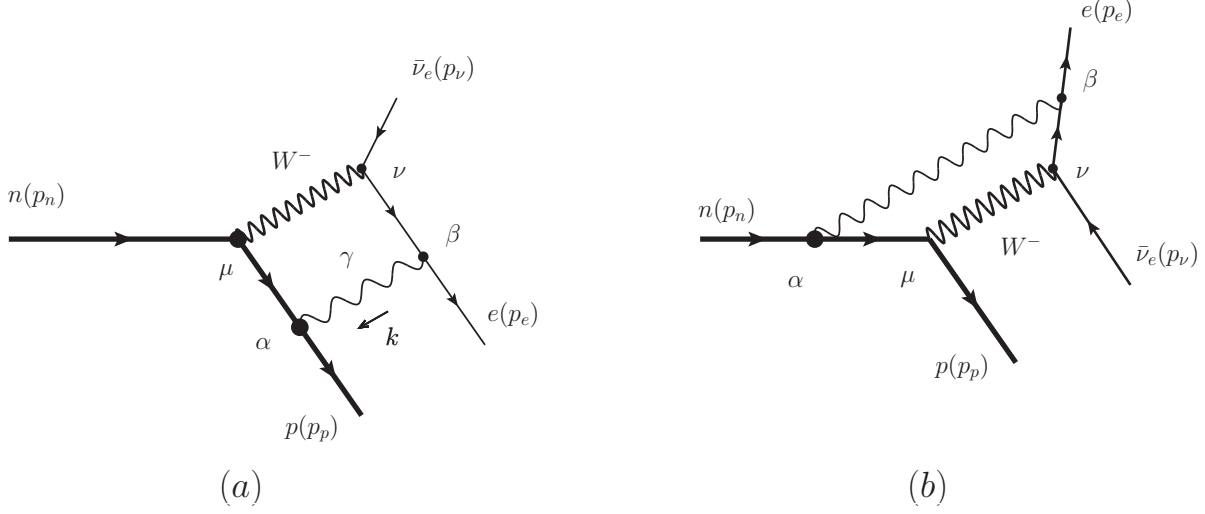


FIG. 2: Diagrams for $n \rightarrow pe\bar{\nu}_e$ under γW -exchange, where only the elastic intermediate states are considered.

means the following replacement:

$$\begin{aligned}
& i\bar{u}(p_e, m_e)\gamma^\beta S_F(p_e + k, m_e)\gamma^\omega(1 - \gamma_5)u(p_\nu, m_\nu) \\
&= \frac{-(2p_e + k)^\beta L^\omega - k^\omega L^\beta + k \cdot L g^{\omega\beta} + i\epsilon^{\beta\omega\rho\sigma} L_\rho k_\sigma}{(p_e + k)^2 - m_e^2} \\
&\rightarrow \frac{i\epsilon^{\beta\omega\rho\sigma} k_\sigma L_\rho}{(p_e + k)^2 - m_e^2},
\end{aligned} \tag{11}$$

where

$$L_\rho \equiv \bar{u}(p_e, m_e)\gamma_\rho(1 - \gamma_5)u(p_\nu, m_\nu). \tag{12}$$

In the following discussion, we only focus on the inner contributions.

B. Approximations used to estimate γW -exchange contributions in literatures

In Refs. [1, 12], the scalar term f_3 and the weak electricity term f_5 are neglected, as these contributions correspond to the second-class currents (SCC). In this work, we also adopt this approximation as follows:

$$\begin{aligned}
f_3(l^2) &\equiv g_S \approx 0, \\
f_5(l^2) &\equiv g_T \approx 0.
\end{aligned} \tag{13}$$

In addition, the following FAL

$$m_n \approx m_p \approx m_N, p_n \approx p_p \approx p, \quad (14)$$

is used in Refs. [1, 12] before loop integration. This means that

$$\bar{u}(p_p, m_p) \Gamma_H^{\mu\alpha}(p_p, p_n, k) u(p_n, m_n) \approx \bar{u}(p, m_N) \Gamma_H^{\mu\alpha}(p, p, k) u(p, m_N), \quad (15)$$

where $\Gamma_H^{\mu\alpha}(p_p, p_n, k)$ refers to hadronic part of $\mathcal{M}_{(a,b)}^{\gamma W}$.

After applying the FAL and the properties of the Dirac equation to simplify the products of Dirac matrices in the hadronic part amplitude, the authors of Ref. [1] further used the following first-class current (FCC) approximation:

$$\begin{aligned} & \bar{u}(p) [\gamma_\mu (\not{p} - \not{k} + M) \gamma_\nu] u(p) \stackrel{\text{FCC}}{=} -i \epsilon_{\mu\rho\nu\sigma} k^\rho \bar{u}(p) \gamma^\sigma \gamma^5 u(p), \\ & \bar{u}(p) \left[\sigma_{\mu\alpha} k^\alpha (\not{p} - \not{k} + m_N) \gamma_\nu u(p) \right] \stackrel{\text{FCC}}{=} 0, \\ & \bar{u}(p) \left[\gamma_\mu (\not{p} - \not{k} + m_N) \sigma_{\nu\alpha} k^\alpha u(p) \right] \stackrel{\text{FCC}}{=} 2m_N \epsilon_{\mu\rho\nu\sigma} k^\rho \bar{u}(p) \gamma^\sigma \gamma^5 u(p), \\ & \bar{u}(p) \left[\sigma_{\mu\beta} k^\beta (\not{p} - \not{k} + M) \sigma_{\nu\alpha} k^\alpha \right] u(p) \stackrel{\text{FCC}}{=} -i (k^2 - 2k \cdot p) \epsilon_{\mu\rho\nu\sigma} k^\rho \bar{u}(p) \gamma^\sigma \gamma^5 u(p), \end{aligned} \quad (16)$$

which can be found in Eqs. (B2a-B2d) of Ref. [1].

C. Non-uniqueness of FCC approximation after applying FAL

As discussed above, in Ref.[1], the properties of the Dirac equation are used to simplify the products of Dirac matrices in the amplitudes after applying the FAL, and then the FCC approximation is applied. In our calculation, we find that such an approach may produce non-uniqueness in the results. Here, we take the left-hand sides of Eqs. (B2b) and (B2c) in Ref.[1] as examples to illustrate the reason for the non-uniqueness. For the left-hand sides of Eqs. (B2b) and (B2c) in Ref. [1], when applying the properties of the Dirac equation to $u(p)$, one obtains the following result, and after the FCC approximation, we have:

$$\begin{aligned} & \bar{u}(p) \left[\sigma_{\mu\alpha} k^\alpha (\not{p} - \not{k} + m_N) \gamma_\nu u(p) \right] \stackrel{\text{FCC}}{=} 0, \\ & \bar{u}(p) \left[\gamma_\mu (\not{p} - \not{k} + m_N) \sigma_{\nu\alpha} k^\alpha u(p) \right] \stackrel{\text{FCC}}{=} 2m_N \epsilon_{\mu\rho\nu\sigma} k^\rho \bar{u}(p) \gamma^\sigma \gamma^5 u(p), \end{aligned} \quad (17)$$

which are the same as Eqs. (B2b) and (B2c) in Ref. [1]. However, when applying the properties of the Dirac equation to $\bar{u}(p)$, one obtains the following result after the FCC approximation:

$$\begin{aligned} & \left[\bar{u}(p) \sigma_{\mu\alpha} k^\alpha (\not{p} - \not{k} + m_N) \gamma_\nu \right] u(p) \stackrel{\text{FCC}}{=} 2m_N \epsilon_{\mu\rho\nu\sigma} k^\rho \bar{u}(p) \gamma^\sigma \gamma^5 u(p), \\ & \left[\bar{u}(p) \gamma_\mu (\not{p} - \not{k} + m_N) \sigma_{\nu\alpha} k^\alpha \right] u(p) \stackrel{\text{FCC}}{=} 0. \end{aligned} \quad (18)$$

In the practical calculation, we find that these two approaches yield different results. The reason for this difference can be traced to the FAL, as the approximation $p_n \approx p_p \approx p$ used in the FAL leads to the left-hand sides of Eqs. (17, 18).

To avoid such non-uniqueness, we do not use the FCC approximation after applying the FAL in the calculation. This means that we only apply the FAL to the hadronic part of the amplitude and neglect the contributions from f_3, f_5 when discussing the inner contributions.

D. The form of the form factors

In practical calculation, the FFs are introduced to simulate real physical interactions. For the EM FFs, the isovector and isoscalar FFs are usually used [1, 12] as follows:

$$F_{1,2}^S \equiv F_{1,2}^{(0)} \equiv F_{1,2}^{(p)} + F_{1,2}^{(n)}, \quad (19)$$

$$F_{1,2}^V \equiv F_{1,2}^{(1)} \equiv F_{1,2}^{(p)} - F_{1,2}^{(n)}. \quad (20)$$

When isospin symmetry is assumed, the contributions from $F_{1,2}^V$ are zero, and only the terms $F_{1,2}^{(S)}$ contribute. Due to this property, a dipole form was directly introduced in Ref. [12] to parameterize the FFs as follows:

$$F_1^{(S)}(l^2) + F_2^{(S)}(l^2) \equiv G_M^{(0)} = (\mu_p + \mu_n) \left(\frac{\Lambda_\gamma^2}{l^2 - \Lambda_\gamma^2} \right)^2, \quad (21)$$

where μ_p and μ_n are the anomalous magnetic moments of the proton and neutron, respectively.

For the weak FFs after assuming SU(2) symmetry and utilizing the conserved-vector-current hypothesis, one obtains:

$$f_{1,2}(l^2) = F_{1,2}^p(l^2) - F_{1,2}^n(l^2). \quad (22)$$

For f_4 , the following simple form is used in Ref. [12] as follows:

$$f_4(l^2) = f_{40}G_D(l^2, \Lambda_W^2), \quad (23)$$

with $f_{40} = g_A$ and

$$G_D(l^2, \Lambda_W^2) \equiv \frac{\Lambda_W^4}{(l^2 - \Lambda_W^2)^2}. \quad (24)$$

The pseudoscalar FF f_6 is not considered, as it does not contribute to the γW -exchange effects in our case.

Since the experimental data sets for the EM FFs of the proton and neutron are independent, we discuss their contributions separately in this work. This separation is also helpful when discussing the contributions beyond the FAL, where isospin symmetry breaking effects should be considered. Furthermore, the physical weak FFs may differ from the dipole form, as shown in Eq. (23). The results using a general form of FFs as inputs will be beneficial for further analysis when more experimental data sets are available in the future. In the practical calculation, we take the FFs as follows:

$$\begin{aligned} F_1^p(l^2) &= F_{10}^p \sum_{j=1}^{N_1} a_{1j} G(l^2, \Lambda_{1j}^2, n_{1j}), \\ F_2^p(l^2) &= F_{20}^p \sum_{j=1}^{N_2} a_{2j} G(l^2, \Lambda_{2j}^2, n_{2j}), \\ F_1^n(l^2) &= F_{10}^n \sum_{j=1}^{N_3} a_{3j} G(l^2, \Lambda_{3j}^2, n_{3j}), \\ F_2^n(l^2) &= F_{20}^n \sum_{j=1}^{N_4} a_{4j} G(l^2, \Lambda_{4j}^2, n_{4j}), \\ f_i(l^2) &= f_{i0} \sum_{j=1}^{\bar{N}_i} b_{ij} G(l^2, \bar{\Lambda}_{ij}^2, \bar{n}_{ij}), \end{aligned} \quad (25)$$

where $F_{10}^p = 1$, $F_{20}^p = \mu_p - 1$, $F_{20}^n = \mu_n$, $f_{10} = g_V = 1$ and $f_{20} = g_M = \mu_p - \mu_n - 1$, N_i , \bar{N}_i , n_{ij} and \bar{n}_{ij} are some positive integer numbers, and

$$G(l^2, \Lambda^2, n) \equiv \frac{(-\Lambda^2)^n}{(l^2 - \Lambda^2)^n}. \quad (26)$$

Also we have the constrained conditions as

$$\begin{aligned}
\sum_{j=1}^{\bar{N}_i} b_{ij} &= 1, \\
\sum_{j=1}^{N_i} a_{ij} &= 1 \quad \text{for } i = 1, 2, 4, \\
\sum_{j=1}^{N_i} a_{3j} &= 0.
\end{aligned} \tag{27}$$

It is easy to verify that these forms of FFs revert to some standard ones with specific values of N_i , \bar{N}_i , \bar{n}_{ij} and n_{ij} . For example, by setting $\bar{N}_4 = 1$, $\bar{n}_{41} = 2$, $\bar{\Lambda}_{41} = \Lambda_W$, and $b_{41} = 1$, f_4 returns to the usual dipole form, as shown in Eq. (23).

III. ANALYTIC RESULTS FOR THE γW -EXCHANGE CONTRIBUTION

To discuss the γW -exchange contributions in a general form, we perform the calculation at the amplitude level rather than at the cross-section level, as is usually done in the literature. To achieve this aim, we reduce the four-dimensional (4D) amplitudes to a two-dimensional (2D) form and express them in the following manner:

$$\mathcal{M}^X \equiv \mathcal{N} \sum_{i=1}^{16} \mathcal{C}_i^X O^i, \tag{28}$$

where

$$\mathcal{N} \equiv -\frac{m_N \sqrt{E_\nu(E_e + m_e)} g^2 V_{ud}}{4m_W^2}, \tag{29}$$

and X refers to W or γW , \mathcal{C}_i are coefficients and O_i are chosen as follows:

$$\begin{aligned}
O_1 &\equiv [\xi_p^\dagger \xi_n][\xi_e^\dagger \boldsymbol{\sigma} \cdot \mathbf{n}_e \eta_\nu], & O_2 &\equiv [\xi_p^\dagger \xi_n][\xi_e^\dagger \boldsymbol{\sigma} \cdot \mathbf{n}_\nu \eta_\nu], \\
O_3 &\equiv [\xi_p^\dagger \xi_n][\xi_e^\dagger \eta_\nu], & O_4 &\equiv [\xi_p^\dagger \xi_n][\xi_e^\dagger \boldsymbol{\sigma} \cdot (\mathbf{n}_e \times \mathbf{n}_\nu) \eta_\nu], \\
O_5 &\equiv [\xi_p^\dagger \boldsymbol{\sigma} \cdot \mathbf{n}_e \xi_n][\xi_e^\dagger \eta_\nu], & O_6 &\equiv [\xi_p^\dagger \boldsymbol{\sigma} \cdot \mathbf{n}_\nu \xi_n][\xi_e^\dagger \eta_\nu], \\
O_7 &\equiv [\xi_p^\dagger \boldsymbol{\sigma} \cdot (\mathbf{n}_e \times \mathbf{n}_\nu) \xi_n][\xi_e^\dagger \boldsymbol{\sigma} \cdot \mathbf{n}_e \eta_\nu], & O_8 &\equiv [\xi_p^\dagger \boldsymbol{\sigma} \cdot (\mathbf{n}_e \times \mathbf{n}_\nu) \xi_n][\xi_e^\dagger \boldsymbol{\sigma} \cdot \mathbf{n}_\nu \eta_\nu], \\
O_9 &\equiv [\xi_p^\dagger \boldsymbol{\sigma} \xi_n] \times [\xi_e^\dagger \boldsymbol{\sigma} \eta_\nu] \cdot \mathbf{n}_e, & O_{10} &\equiv [\xi_p^\dagger \boldsymbol{\sigma} \xi_n] \times [\xi_e^\dagger \boldsymbol{\sigma} \eta_\nu] \cdot \mathbf{n}_\nu, \\
O_{11} &\equiv [\xi_p^\dagger \boldsymbol{\sigma} \cdot \xi_n] \cdot [\xi_e^\dagger \boldsymbol{\sigma} \eta_\nu], & O_{12} &\equiv [\xi_p^\dagger \boldsymbol{\sigma} \cdot \mathbf{n}_e \xi_n][\xi_e^\dagger \boldsymbol{\sigma} \cdot \mathbf{n}_e \eta_\nu], \\
O_{13} &\equiv [\xi_p^\dagger \boldsymbol{\sigma} \cdot \mathbf{n}_e \xi_n][\xi_e^\dagger \boldsymbol{\sigma} \cdot \mathbf{n}_\nu \eta_\nu], & O_{14} &\equiv [\xi_p^\dagger \boldsymbol{\sigma} \cdot \mathbf{n}_\nu \xi_n][\xi_e^\dagger \boldsymbol{\sigma} \cdot \mathbf{n}_e \eta_\nu], \\
O_{15} &\equiv [\xi_p^\dagger \boldsymbol{\sigma} \cdot \mathbf{n}_\nu \xi_n][\xi_e^\dagger \boldsymbol{\sigma} \cdot \mathbf{n}_\nu \eta_\nu], & O_{16} &\equiv [\xi_p^\dagger \boldsymbol{\sigma} \cdot (\mathbf{n}_e \times \mathbf{n}_\nu) \xi_n][\xi_e^\dagger \eta_\nu].
\end{aligned} \tag{30}$$

Here ξ, η are the Pauli spinors of particle and anti-particle with corresponding helicity, and $\boldsymbol{\sigma}$ is the Pauli matrix. The unit vectors \mathbf{n}_e and \mathbf{n}_ν are oriented along the direction of the electron's three-momentum \mathbf{p}_e and antineutrino's three-momentum \mathbf{p}_ν , respectively.

Furthermore, one can separate the amplitudes into Fermi (F) part and Gamow-Teller (GT) part as

$$\begin{aligned}
\mathcal{M}^X &\equiv \mathcal{M}_F^X + \mathcal{M}_{GT}^X, \\
\mathcal{M}_F^X &\equiv \mathcal{N} \sum_{i=1}^4 \mathcal{C}_i^X O^i, \\
\mathcal{M}_{GT}^X &\equiv \mathcal{N} \sum_{i=5}^{16} \mathcal{C}_i^X O^i.
\end{aligned} \tag{31}$$

In the practical calculation, we approximately take the antineutrino mass as $m_\nu \approx 0$ and use the package FeynCalc [20] to handle the Dirac matrices in four dimensions, the package PackageX [21] to perform the loop integration, and the package LoopTools [22] for double-checking.

For the one- W -exchange contribution, we first calculate the amplitude beyond the FAL and then expand the coefficients \mathcal{C}_i^W in terms of m_W^{-1} and m_n^{-1} to the leading order (LO). Finally we get

$$\begin{aligned}
\mathcal{C}_{2,LO}^W &= -\mathcal{C}_{3,LO}^W = g_V, \\
\mathcal{C}_{6,LO}^W &= i\mathcal{C}_{10,LO}^W = -\mathcal{C}_{11,LO}^W = g_A,
\end{aligned} \tag{32}$$

and other 11 coefficients are zero at LO.

For the γW -exchange contribution, we first apply the FAL to the 4D amplitude, excluding the Dirac spinors, before performing the loop integration. Next, we reduce the 4D amplitude to its 2D form, keeping $\mathbf{p}_e, \mathbf{p}_\nu$ and m_e in Dirac spinors as non-zero. We then utilize the package PackageX [21] to conduct the loop integration. Finally, we treat $m_W^{-1}, |\mathbf{p}_e|, |\mathbf{p}_\nu|$, and m_e as small quantities and expand $\mathcal{C}_i^{\gamma W}$ in terms of these small variables to LO. Similarly, we find that only $\mathcal{C}_{2,3,6,10,11}^{\gamma W}$ are non-zero at LO in the small variables, and they can be expressed as:

$$\begin{aligned}\mathcal{C}_{2,LO}^{\gamma W} &= \frac{\alpha_e g_A}{8\pi} [d_{2,1} F_{10}^p + d_{2,2} F_{20}^p + d_{2,3} F_{10}^n + d_{2,4} F_{20}^n], \\ \mathcal{C}_{6,LO}^{\gamma W} &= \frac{\alpha_e g_V}{8\pi} [d_{6,1}^V F_{10}^p + d_{6,2}^V F_{20}^p + d_{6,3}^V F_{10}^n + d_{6,4}^V F_{20}^n] \\ &\quad + \frac{\alpha_e g_M}{8\pi} [d_{6,1}^M F_{10}^p + d_{6,2}^M F_{20}^p + d_{6,3}^M F_{10}^n + d_{6,4}^M F_{20}^n],\end{aligned}\tag{33}$$

where

$$d_{2,i} = \sum_{j,k} \hat{\mathcal{F}}_{ij,4k} \left[\frac{X_1(\Lambda_{ij}, \Lambda_{4k})}{2m_N^4(\Lambda_{ij}^2 - \Lambda_{4k}^2)} - \frac{\Lambda_{ij} Z_1(\Lambda_{4k}) - \Lambda_{4k} Z_1(\Lambda_{ij})}{m_N^4 \Lambda_{ij} \Lambda_{4k} (\Lambda_{ij}^2 - \Lambda_{4k}^2)} \right],\tag{34}$$

and

$$\begin{aligned}d_{6,1}^V &= \sum_{j,k} \hat{\mathcal{F}}_{1j,1k} \left[\frac{X_2(\Lambda_{1j}, \Lambda_{1k})}{6m_N^4(\Lambda_{1j}^2 - \Lambda_{1k}^2)} + \frac{\Lambda_{1j} Z_2(\Lambda_{1k}) - \Lambda_{1k} Z_2(\Lambda_{1j})}{3m_N^4 \Lambda_{1j} \Lambda_{1k} (\Lambda_{1j}^2 - \Lambda_{1k}^2)} \right], \\ d_{6,2}^V &= \sum_{j,k} \hat{\mathcal{F}}_{2j,1k} \left[\frac{X_3(\Lambda_{2j}, \Lambda_{1k})}{3m_N^4(\Lambda_{2j}^2 - \Lambda_{1k}^2)} + \frac{2[\Lambda_{2j} Z_3(\Lambda_{1k}) - \Lambda_{1k} Z_3(\Lambda_{2j})]}{3m_N^4 \Lambda_{2j} \Lambda_{1k} (\Lambda_{2j}^2 - \Lambda_{1k}^2)} \right], \\ d_{6,3}^V &= [d_{6,1}^V \text{ after replacing the index } 1j \text{ with } 3j], \\ d_{6,4}^V &= [d_{6,2}^V \text{ after replacing the index } 2j \text{ with } 4j],\end{aligned}\tag{35}$$

and

$$\begin{aligned}d_{6,1}^M &= [d_{6,2}^V \text{ after replacing the indexes } 2j \text{ and } 1k \text{ with } 1j \text{ and } 2k, \text{ respectively}], \\ d_{6,2}^M &= \sum_{j,k} \hat{\mathcal{F}}_{2j,2k} \left[\frac{X_4(\Lambda_{2j}, \Lambda_{2k})}{4m_N^4(\Lambda_{2j}^2 - \Lambda_{2k}^2)} - \frac{Z_4(\Lambda_{2k}) - Z_4(\Lambda_{2j})}{m_N^4(\Lambda_{2j}^2 - \Lambda_{2k}^2)} \right], \\ d_{6,3}^M &= [d_{6,1}^M \text{ after replacing the index } 1j \text{ with } 3j], \\ d_{6,4}^M &= [d_{6,2}^M \text{ after replacing the index } 2j \text{ with } 4j].\end{aligned}\tag{36}$$

Here the operator $\hat{\mathcal{F}}_{ij,mk}$ is defined as

$$\hat{\mathcal{F}}_{ij,mk} \equiv a_{ij} b_{mk} \Lambda_{ij}^{2n_{ij}} \bar{\Lambda}_{mk}^{2\bar{n}_{mk}} \frac{(-1)^{n_{ij} + \bar{n}_{mk}}}{(n_{ij} - 1)! (\bar{n}_{mk} - 1)!} \frac{d^{n_{ij} - 1}}{d(\Lambda_{ij}^2)^{n_{ij} - 1}} \frac{d^{\bar{n}_{mk} - 1}}{d(\bar{\Lambda}_{mk}^2)^{\bar{n}_{mk} - 1}}, \quad (37)$$

and the functions X_i, Y, Z_i are defined as

$$\begin{aligned} X_1(x, y) &\equiv x^2 \log \frac{m_N^2}{x^2} - y^2 \log \frac{m_N^2}{y^2} + 6m_N^2 \log \frac{x^2}{y^2}, \\ X_2(x, y) &\equiv -x^2 \log \frac{m_N^2}{x^2} + y^2 \log \frac{m_N^2}{y^2} + 6m_N^2 \log \frac{x^2}{y^2}, \\ X_3(x, y) &\equiv x^2 \log \frac{m_N^2}{x^2} - y^2 \log \frac{m_N^2}{y^2}, \\ X_4(x, y) &\equiv -2x^2 \log \frac{m_N^2}{x^2} + 2y^2 \log \frac{m_N^2}{y^2} - m_N^2 \log \frac{x^2}{y^2}, \\ Y(x) &\equiv \log \left[\frac{x + \sqrt{-4m_N^2 + x^2}}{2m_N} \right], \\ Z_1(x) &\equiv (-4m_N^2 + x^2)^{3/2} Y(x), \\ Z_2(x) &\equiv (-4m_N^2 + x^2)^{1/2} (8m_N^2 + x^2) Y(x), \\ Z_3(x) &\equiv (-4m_N^2 + x^2)^{1/2} (2m_N^2 + x^2) Y(x), \\ Z_4(x) &\equiv (-4m_N^2 + x^2)^{1/2} x Y(x). \end{aligned} \quad (38)$$

In addition, the following relations are also obtained:

$$d_{3,j} = -d_{2,j}, \quad d_{10,j} = -id_{6,j}, \quad d_{11,j} = -d_{6,j}, \quad (39)$$

with $j = 1, 2, 3, 4$.

We would like to note that for denominators such as $\Lambda_{ij}^2 - \Lambda_{4k}^2$ in the expressions d_{ij} , the limit $\Lambda_{ij} \rightarrow \Lambda_{4k}$ is understood when $\Lambda_{ij} = \Lambda_{4k}$.

From the above expression, we can define the γW -exchange corrections as:

$$\frac{\alpha_e}{2\pi} \delta_i \equiv \frac{C_{i,LO}^{\gamma W}}{C_{i,LO}^W}. \quad (40)$$

It is easy to verify that the corrections $C_{\text{Born}}^{\text{F/GT}}$ defined in Refs. [1, 12] can be expressed as

$$\begin{aligned} C_{\text{Born}}^{\text{F}} &= \delta_2 = \delta_3, \\ C_{\text{Born}}^{\text{GT}} &= \delta_6 = \delta_{10} = \delta_{11}. \end{aligned} \quad (41)$$

For simplicity, we also separate $C_{\text{Born}}^{\text{F,GT}}$ into two parts as:

$$\begin{aligned} C_{\text{Born}}^{\text{F}} &\equiv C_{\text{Born}}^{\text{F},g_A} + C_{\text{Born}}^{\text{F},g_M}, \\ C_{\text{Born}}^{\text{GT}} &\equiv C_{\text{Born}}^{\text{GT},g_V} + C_{\text{Born}}^{\text{GT},g_M}, \end{aligned} \quad (42)$$

where the indexes $g_{A,V,M}$ refer to the contributions from $g_{A,V,M}$ in the γW -exchange contributions, respectively. We would like to mention that $C_{\text{Born}}^{\text{F},g_M}$ is zero and we will not be considered this in the following discussion.

IV. NUMERICAL COMPARISON AND DISCUSSIONS

A. Numerical inputs

To provide a clear picture of the γW -exchange corrections, we present the numerical results in this section where the following masses and coupling constants are used

$$\begin{aligned} m_n &= 939.56542 \text{ MeV}, m_p = 938.27209 \text{ MeV}, m_e = 0.51100 \text{ MeV}, \\ F_{10}^p &= 1, F_{20}^p = 1.793, F_{20}^n = -1.913, \\ g_V &= 1, g_A = -1.26, g_M = F_{20}^p - F_{20}^n = 3.706. \end{aligned} \quad (43)$$

For the EM FFs of proton and neutron, $F_{1,2}^{p,n}$, perturbative theory suggests that

$$\begin{aligned} F_1^{p,n}(Q^2 \rightarrow \infty) &\propto \frac{1}{Q^4}, \\ F_2^{p,n}(Q^2 \rightarrow \infty) &\propto \frac{1}{Q^6}, \end{aligned} \quad (44)$$

so we choose the following N_i and corresponding n_{ij} in Eq. (27) as

$$N_i = 2, \quad n_{11,12,31,32} = 2, \quad n_{21,22,41,42} = 3. \quad (45)$$

We fit the parameters a_{ij} and Λ_{ij} in $F_{1,2}^p$ using the experimental datasets from Ref. [23] and fit the corresponding parameters in $F_{1,2}^n$ using the formulas from Ref. [24]. Finally, we

choose the parameters as follows:

$$\begin{aligned}
N_1 &= 2, n_{1j} = 2, a_{11} = 0.609, \Lambda_{11} = 0.815, a_{12} = 0.391, \Lambda_{12} = 1.230, \\
N_2 &= 2, n_{2j} = 3, a_{21} = 0.858, \Lambda_{21} = 0.970, a_{22} = 0.142, \Lambda_{22} = 1.598, \\
N_3 &= 2, n_{3j} = 2, a_{31} = 1, \Lambda_{31} = 1.288, a_{32} = -1, \Lambda_{32} = 1.378, F_{10}^n = 1, \\
N_4 &= 2, n_{4j} = 3, a_{41} = 0.348, \Lambda_{41} = 0.699, a_{42} = 0.652, \Lambda_{42} = 1.214,
\end{aligned} \tag{46}$$

where $j = 1, 2$, the unit of Λ_{ij} is GeV while a_{ij} is dimensionless.

We would like to mention that the γW -exchange contributions from the elastic intermediate state are not sensitive to the behavior of FFs in very high energy, therefore we do not apply the following constraint condition:

$$\mu_p G_E^p / G_M^p \xrightarrow{Q^2 \rightarrow \infty} 1, \tag{47}$$

where

$$\begin{aligned}
G_M^{p,n}(Q^2) &\equiv F_1^{p,n}(Q^2) + F_2^{p,n}(Q^2), \\
G_E^{p,n}(Q^2) &\equiv F_1^{p,n}(Q^2) - \frac{Q^2}{4m_{p,n}^2} F_2^{p,n}(Q^2).
\end{aligned} \tag{48}$$

For comparison, we also use the following simple forms for the EM FFs as inputs to present the results

$$\begin{aligned}
N_1 &= 1, n_{11} = 2, a_{11} = 1, \Lambda_{11} = 1.006, \\
N_2 &= 1, n_{21} = 3, a_{21} = 1, \Lambda_{21} = 1.123, \\
N_3 &= 2, n_{3j} = 1, a_{31} = 1, \Lambda_{31} = 0.847, a_{32} = -1, \Lambda_{32} = 0.914, F_{10}^n = 1, \\
N_4 &= 1, n_{41} = 3, a_{41} = 1, \Lambda_{41} = 1.038.
\end{aligned} \tag{49}$$

Naively, the EM FFs used in Ref. [12] correspond to the following choices:

$$N_i = 1, n_{i1} = 2, a_{i1} = 1, \Lambda_{i1} = \Lambda_\gamma = 0.84, F_{10}^n = 0, \tag{50}$$

with $i = 1, 2, 3, 4$.

In the following, we name the choices of the EM FFs and cut-offs by Eqs. (46, 49, 50) as types I, II and III, respectively. A detailed comparison of the corresponding EM FFs

$G_{E,M}^{p,n}$ and the fits in Ref. [24] is presented in Figs. 3, 4, where the world datasets for $G_{E,M}^p$ [23], G_E^n [25–39] and G_M^n [40–53] are also included. The comparisons in Fig. 3 show that, globally, the $G_{E,M}^p$ in types I and II and the fits in Ref. [24] are highly consistent with experimental datasets in the region $Q^2 \subset [0, 6]$ GeV², while the $G_{E,M}^p$ in type III is slightly underestimated. The comparisons in Fig. 4 indicate that the $G_{E,M}^n$ in type I and the fits in Ref. [24] are consistent with the experimental datasets, while the $G_{E,M}^n$ in types II and III show some discrepancies. Since, in practical calculations, the EM FFs $F_{1,2}^{p,n}$ are used and the results are somewhat sensitive to their low energy-behaviors, we show the corresponding behaviors in Fig. 5. In this figure we can see that the FFs $F_{1,2}^p$ and F_2^n in type I are almost the same as the fits in Ref. [24], while the other results differ slightly from those fits in Ref. [24]. We will demonstrate that these differences lead to variations in the corresponding C_{Born} .

For the weak FFs $f_{1,2}(Q^2)$, we assume the isospin symmetry and use Eq. (22) to derive $f_{1,2}(Q^2)$ from the EM FFs $F_{1,2}^{p,n}(Q^2)$. Once $F_{1,2}^{p,n}(Q^2)$ are known, all the parameters in $f_{1,2}(Q^2)$, such as b_{ij} and $\bar{\Lambda}_{ij}$, are fixed. The only unknown is $f_4(Q^2)$. Since the experimental datasets for $f_4(Q^2)$ are insufficient, we simply take them to be the same as those used in Ref. [12], which corresponds to the following special choices in Eq. (27):

$$\bar{N}_4 = 1, \bar{n}_{41} = 2, b_{41} = 1, \bar{\Lambda}_{41} = \Lambda_W = 1.09 \pm 0.05 \text{ GeV}. \quad (51)$$

In principle, one can choose more general forms for f_4 using Eq. (27) when the experimental datasets are sufficiently robust. Here, we simply take it as an example for comparison.

B. Numerical Results for C_{Born}

By using the types I, II and III FFs as inputs, we list the final numerical results for C_{Born} in Tab. I, where we have maintained a precision of 0.1%. However, we would like to emphasize that the recoil contributions beyond the FAL in the γW -exchange will result in a difference of approximately parts-per-thousand. In Ref. [12], the parameters used in FFs are the same as those in Eq. (50). In Ref. [1], the global fit results of Ref. [24] for nucleon magnetic Sachs FFs and the model-independent z-expansion analysis of Ref. [54] for the axial form factor were utilized. For comparison, we presented these two related results and

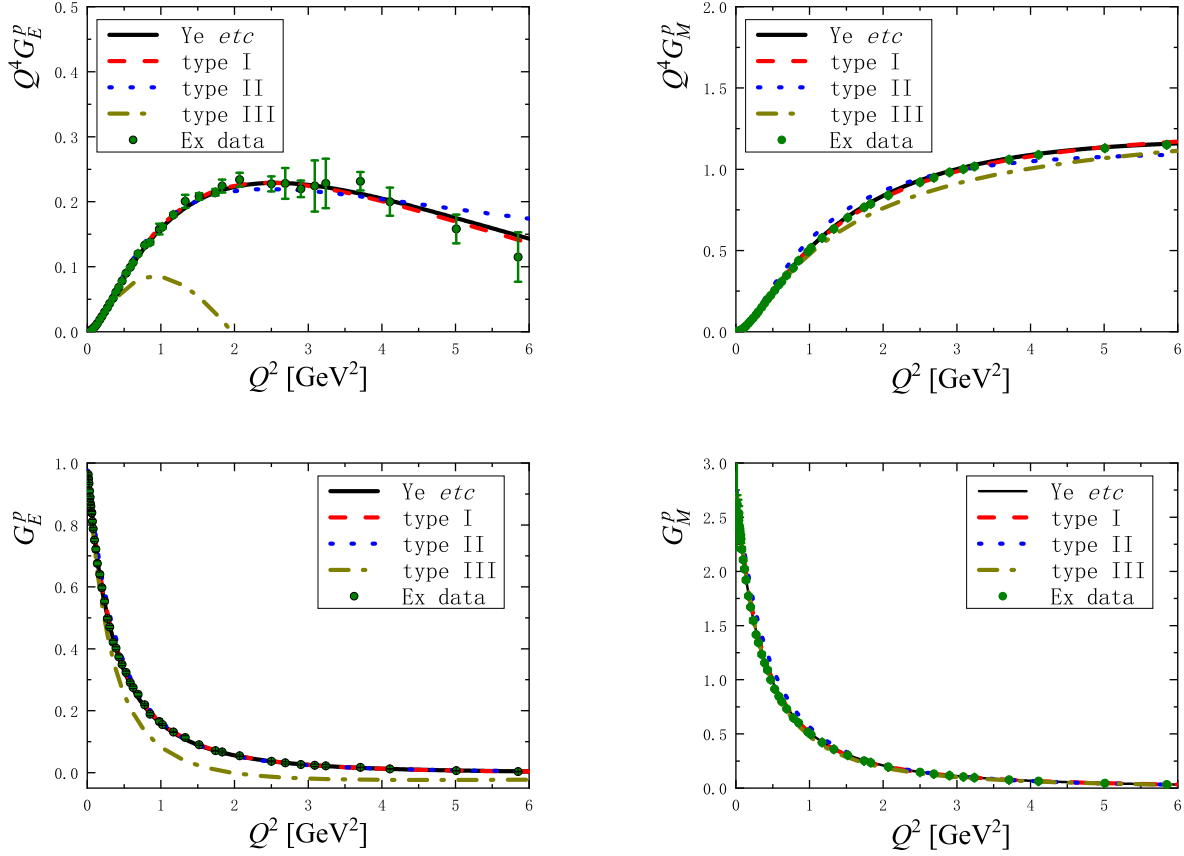


FIG. 3: Numerical comparison for the EM FFs of proton $G_{E,M}^p$ with different parameters. The above panel is for $Q^4 G_{E,M}^p(Q^2)$ vs. Q^2 and the bottom panel is for $G_{E,M}^p(Q^2)$ vs. Q^2 . The results labelled by *Ye etc* refer to the fitted results in Ref. [24]. The type I, II, III are corresponding to the choices of parameters by Eqs. (46, 49, 50), respectively. The experimental data sets for $G_{E,M}^p$ are taken from Ref. [23].

our results in Tab. I.

In Tab. I, one can see that the results for $C_{\text{Born}}^{\text{F},gA}$ with types I and III EM FFs are consistent with those given in Refs. [1, 12] within the error, while the corresponding result with type II EM FFs are slightly larger. In contrast to the case of $C_{\text{Born}}^{\text{F},gA}$, our results (type I) for $C_{\text{Born}}^{\text{GT},gV}$ and $C_{\text{Born}}^{\text{GT},gM}$ are about 13% and 7% larger than those reported in Ref. [1], respectively. The comparisons of the results for $C_{\text{Born}}^{\text{GT},gV}$ from types I, II, and III suggest that the results are somewhat sensitive to the choices of the EM FFs. The comparisons of the results for $C_{\text{Born}}^{\text{GT},gM}$

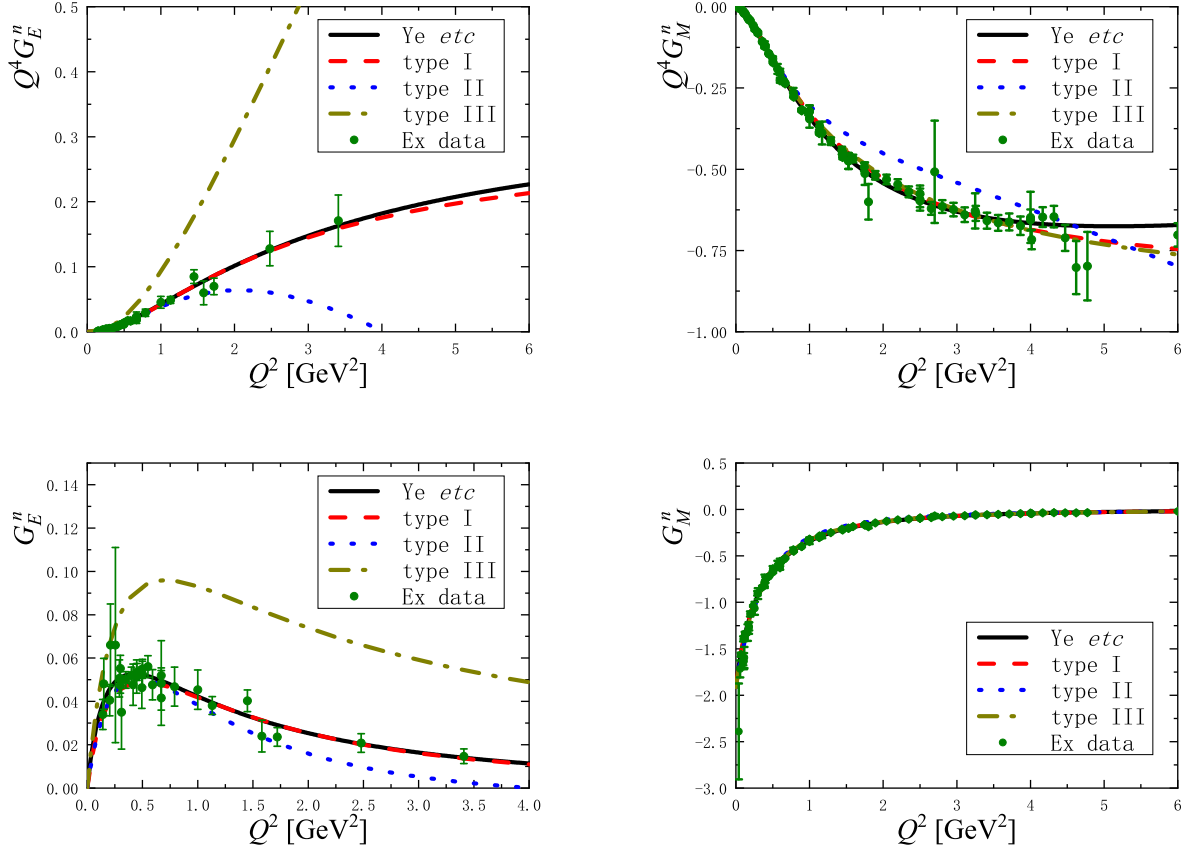


FIG. 4: Numerical comparison for the EM FFs of neutron $G_{E,M}^n$ with different parameters. The above panel is for $Q^4 G_{E,M}^n(Q^2)$ vs. Q^2 and the bottom panel is for $G_{E,M}^n(Q^2)$ vs. Q^2 . The results labelled by *Ye etc* refer to the fitted results in Ref. [24]. The type I, II, III are corresponding to the choices of parameters by Eqs. (46, 49, 50), respectively. The data sets for $G_E^n(Q^2)$ are taken from Refs. [25–39]. The experimental data sets for $G_M^n(Q^2)$ are taken from Refs. [40–53].

from types I, II, III with that in Ref. [1] indicate that their difference is not due to the choices of FFs. A possible reason for this discrepancy is the use of the FCC approximation. As discussed above, the naive FCC approximation is non-unique. In our practical calculations, we also choose different forms of the FCC approximation as examples for comparison and find that the results vary.

To present the contributions more clearly, we also separate the contributions from different

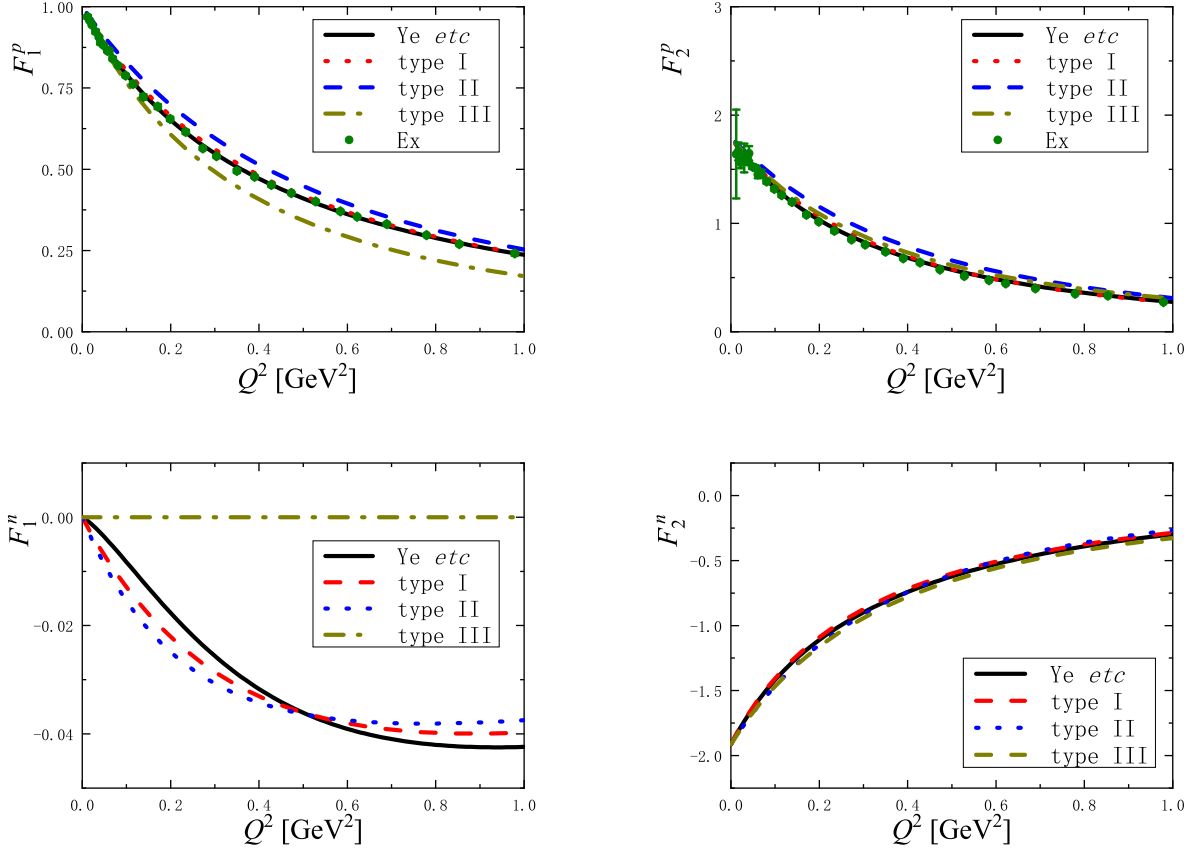


FIG. 5: Numerical comparison for the EM FF $F_{1,2}^{p,n}$ with different parameters. The above panel is for $F_{1,2}^p(Q^2)$ vs. Q^2 and the bottom panel is for $F_{1,2}^n$ vs. Q^2 . The results labelled by *Ye etc* refer to the fitted results in Ref. [24]. The type I, II, III are corresponding to the choices of parameters by Eqs. (46, 49, 50), respectively. The data sets for $F_{1,2}^p$ are combined from the experimental data sets $G_{E,M}^p(Q^2)$ from Ref. [23]. The data sets for $F_{1,2}^n$ are not presented.

parts, which are expressed as follows:

$$\text{type I: } \begin{cases} C_{\text{Born}}^{F, gA} = 1.058F_{10}^p + 0.985F_{20}^p - 0.027F_{10}^n + 0.966F_{20}^n = 0.951, \\ C_{\text{Born}}^{\text{GT}, gV} = 0.473F_{10}^p + 0.238F_{20}^p - 0.013F_{10}^n + 0.233F_{20}^n = 0.442, \\ C_{\text{Born}}^{\text{GT}, gM} = 0.853F_{10}^p - 0.019F_{20}^p - 0.019F_{10}^n - 0.019F_{20}^n = 0.835, \end{cases} \quad (52)$$

	FFs	$C_{\text{Born}}^{\text{F},gA}$	$C_{\text{Born}}^{\text{GT},gV}$	$C_{\text{Born}}^{\text{GT},gM}$
Ref. [12]	Eqs. (27, 51, 49)	0.881 ± 0.014	no calculated	no calculated
Ref. [1]	Refs. [24, 54]	0.91(5)	0.39(1)	0.78(2)
type I	Eqs. (27, 51, 46)	0.951	0.442	0.835
type II	Eqs. (27, 51, 49)	1.009	0.475	0.876
type III	Eqs. (27, 51, 50)	0.882	0.388	0.832

TABLE I: The numerical results for C_{Born} in Refs. [1, 12] and this work.

and

$$\text{type II : } \begin{cases} C_{\text{Born}}^{\text{F},gA} = 1.084F_{10}^p + 1.024F_{20}^p - 0.028F_{10}^n + 0.985F_{20}^n = 1.009, \\ C_{\text{Born}}^{\text{GT},gV} = 0.498F_{10}^p + 0.255F_{20}^p - 0.014F_{10}^n + 0.244F_{20}^n = 0.475, \\ C_{\text{Born}}^{\text{GT},gM} = 0.901F_{10}^p - 0.024F_{20}^p - 0.021F_{10}^n - 0.020F_{20}^n = 0.876, \end{cases} \quad (53)$$

and

$$\text{type III : } \begin{cases} C_{\text{Born}}^{\text{F},gA} = 0.999F_{10}^p + 0.999F_{20}^p + 0.999F_{20}^n = 0.882, \\ C_{\text{Born}}^{\text{GT},gV} = 0.414F_{10}^p + 0.224F_{20}^p + 0.224F_{20}^n = 0.388, \\ C_{\text{Born}}^{\text{GT},gM} = 0.829F_{10}^p - 0.024F_{20}^p - 0.024F_{20}^n = 0.832. \end{cases} \quad (54)$$

The results in Eqs. (52, 53, 54) show that the EM FF F_1^p contributes the most significantly to $C_{\text{Born}}^{\text{GT}}$. The comparison among these results indicates that they are somewhat sensitive to the cutoff in F_1^p . The differences can be traced to the varying behaviors of $F_{1,2}^{p,n}$ presented in Fig. 5. For example, the F_1^p in type II case is slightly larger than that in type I, which results in the contributions from type II being larger than those from I and III. There is about 5% – 13% difference due to the different parameterizations of the EM FFs. In this work, we favor the type I case.

Furthermore, we list the relative ratios of the contributions from different EM FFs in Tab. II. It clearly shows that contributions from $F_1^p, F_2^{p,n}$ are significant for $C_{\text{Born}}^{\text{F},gA}$ and $C_{\text{Born}}^{\text{GT},gV}$. Additionally, there are substantial cancellations between F_2^p and F_2^n . The contributions from F_1^n are of the same order as the sum of F_2^p and F_2^n , accounting for a few percent of the full corrections. These properties indicate that the precise measurements of $F_{1,2}^n$ are crucial for achieving an accurate estimation of the γW -exchange contributions. Another interesting observation is that the contributions to $C_{\text{Born}}^{\text{GT},gM}$ primarily come from F_1^p .

contributions/All	$C_{\text{Born}}^{\text{F},g_A}(f_4)$	$C_{\text{Born}}^{\text{GT},g_V}(f_1)$	$C_{\text{Born}}^{\text{GT},g_M}(f_2)$
F_1^p	111%	107%	102%
F_2^p	186%	97%	-4%
F_1^n	-3%	-3%	-2%
F_2^n	-194%	-100%	4%

TABLE II: The ratios of the different contributions in type I case.

In Fig. 6, we present the numerical results for the dependence of $C_{\text{Born}}^{\text{F,GT}}$ on Λ_{11} in type I case with $\Lambda_{12} = \Lambda_{11}$. It can be observed that the results are somewhat sensitive to the cutoff. Naively, when the cutoff $\Lambda_{12} = \Lambda_{11} \rightarrow \infty$, the results with $F_{20}^p = 0$ should revert to the point-like particle case. The large difference between the results with the physical Λ_{ij} and ∞ indicates that, although neutron β decay is a low energy process, the internal structure remains crucial for estimating the γW -exchange contribution. This property also suggests that the naive power counting of the low-energy effective theory should be applied with caution in neutron β decay.

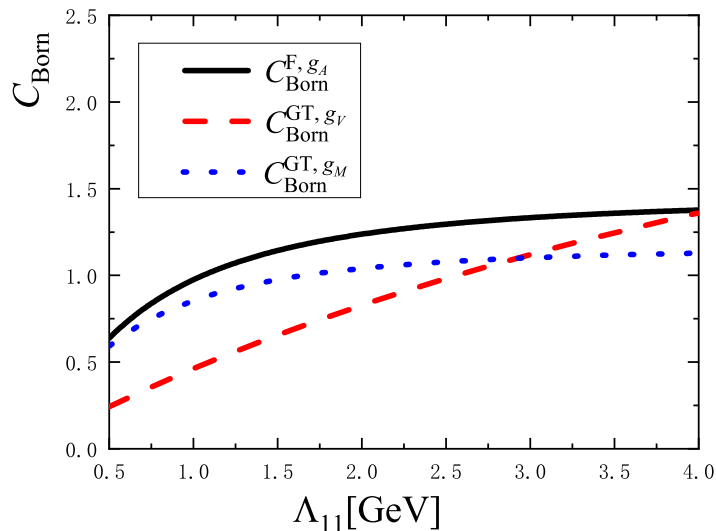


FIG. 6: Numeric results for C_{Born} vs. Λ_{11} where the type I EM FFs and $\Lambda_{12} = \Lambda_{11}$ are used.

V. SUMMARY

In summary, the γW -exchange contributions with the elastic intermediate state in neutron β decay are discussed at the amplitude level in the FAL. The non-uniqueness in the usual FAL and FCC approximations is addressed. To avoid this non-uniqueness, we first perform the full calculation at the amplitude level and then separate the contributions into inner and outer parts.

The analytical results for the γW -exchange contribution are presented with a general form for the EM FFs of the proton and neutron as inputs. The parameters in this general form of the form factors can be determined by future precise experimental data sets, and the derived analytical expressions are helpful for analyzing the uncertainty.

By fitting with the current experimental datasets for the EM FFs, our numeric results for $C_{\text{Born}}^{\text{F},gA}$ are consistent with those presented in Refs. [1, 12]. Additionally, our numerical results for $C_{\text{Born}}^{\text{GT},gV}$ and $C_{\text{Born}}^{\text{GT},gM}$ are approximately 13% and 7% larger than those reported in Ref. [1]. The contributions from different parts of the EM FFs are also discussed, and these results indicate that to achieve a precise estimation of the γW -exchange contribution, the precise EM FFs for neutron is needed.

VI. ACKNOWLEDGMENTS

H. Q. Zhou would like to thank Zhi-Hui Guo for helpful discussions. H. Q. Zhou is supported by the National Natural Science Foundation of China under Grants Nos. 12150013 and 12075058. H. Y. Cao is supported by the Science and Technology Research Project of Hubei Provincial Education Department under Grants No. Q20222502 and by the National Natural Science Foundation of China under Grants No. 12405153.

-
- [1] L. Hayen, Phys. Rev. D **103**, 113001 (2021).
 - [2] S. Navas et al. (Particle Data Group), Phys. Rev. D **110**, 030001 (2024).
 - [3] H. Abele et al., Phys. Rev. Lett. **88**, 211801 (2002).
 - [4] D. Dubbers and M. G. Schmidt, Rev. Mod. Phys. **83**, 1111 (2011).

- [5] F. E. Wietfeldt and G. L. Greene, *Rev. Mod. Phys.* **83**, 1173 (2011).
- [6] N. Severijns and O. Naviliat-Cuncic, *Ann. Rev. Nucl. Part. Sci.* **61**, 23 (2011).
- [7] C. Y. Seng, *Particles* **4**, 397 (2021).
- [8] A. Sirlin, *Phys. Rev.* **164**, 1767 (1967).
- [9] A. Sirlin, *Rev. Mod. Phys.* **50**, 573 (1978), [Erratum: *Rev. Mod. Phys.* **50**, 905 (1978)].
- [10] A. Czarnecki, W. J. Marciano, and A. Sirlin, *Phys. Rev. D* **70**, 093006 (2004).
- [11] W. J. Marciano and A. Sirlin, *Phys. Rev. Lett.* **96**, 032002 (2006).
- [12] I. S. Towner, *Nucl. Phys. A* **540**, 478 (1992).
- [13] C. Y. Seng et al., *Phys. Rev. Lett.* **121**, 241804 (2018).
- [14] C. Y. Seng, M. Gorchtein, and M. J. Ramsey-Musolf, *Phys. Rev. D* **100**, 013001 (2019).
- [15] M. Gorchtein and C. Y. Seng, *JHEP* **10**, 053 (2021).
- [16] P. X. Ma et al., *Phys. Rev. Lett.* **132**, 191901 (2024).
- [17] O. Tomalak and M. Vanderhaeghen, *Eur. Phys. J. A* **51**, 24 (2015), 1408.5330.
- [18] H. Y. Cao and H. Q. Zhou, *Chin. Phys. C* **45**, 073106 (2021), 2005.08265.
- [19] Q. Q. Guo and H. Q. Zhou, *Phys. Rev. C* **109**, 014308 (2024).
- [20] V. Shtabovenko, R. Mertig, and F. Orellana, *Comput. Phys. Commun.* **256**, 107478 (2020).
- [21] H. H. Patel, *Comput. Phys. Commun.* **197**, 276 (2015).
- [22] T. Hahn and M. Perez-Victoria, *Comput. Phys. Commun.* **118**, 153 (1999).
- [23] J. Arrington, W. Melnitchouk, and J. A. Tjon, *Phys. Rev. C* **76**, 035205 (2007).
- [24] Z. Ye et al., *Phys. Lett. B* **777**, 8 (2018).
- [25] M. Meyerhoff et al., *Physics Letters B* **327**, 201 (1994), ISSN 0370-2693.
- [26] T. Eden et al., *Phys. Rev. C* **50**, R1749 (1994).
- [27] I. Passchier et al., *Phys. Rev. Lett.* **82**, 4988 (1999).
- [28] C. Herberg et al., *Eur. Phys. J. A* **5**, 131 (1999).
- [29] D. Rohe et al., *Phys. Rev. Lett.* **83**, 4257 (1999).
- [30] J. Golak et al., *Phys. Rev. C* **63**, 034006 (2001).
- [31] H. Zhu et al. (E93026), *Phys. Rev. Lett.* **87**, 081801 (2001).
- [32] J. Bermuth et al., *Phys. Lett. B* **564**, 199 (2003).
- [33] R. Madey et al. (E93-038), *Phys. Rev. Lett.* **91**, 122002 (2003).

- [34] G. Warren et al. (Jefferson Lab E93-026), Phys. Rev. Lett. **92**, 042301 (2004).
- [35] D. I. Glazier et al., Eur. Phys. J. A **24**, 101 (2005).
- [36] E. Geis et al. (BLAST), Phys. Rev. Lett. **101**, 042501 (2008).
- [37] S. Riordan et al., Phys. Rev. Lett. **105**, 262302 (2010).
- [38] B. S. Schlimme et al., Phys. Rev. Lett. **111**, 132504 (2013).
- [39] J. Bermuth et al., Phys. Lett. B **564**, 199 (2003).
- [40] S. Rock et al., Phys. Rev. Lett. **49**, 1139 (1982).
- [41] A. Lung et al., Phys. Rev. Lett. **70**, 718 (1993).
- [42] H. Anklin et al., Phys. Lett. B **428**, 248 (1998).
- [43] G. Kubon et al., Phys. Lett. B **524**, 26 (2002).
- [44] B. Anderson et al. (Jefferson Lab E95-001), Phys. Rev. C **75**, 034003 (2007).
- [45] J. Lachniet et al. (CLAS), Phys. Rev. Lett. **102**, 192001 (2009).
- [46] W. Bartel et al., Nucl. Phys. B **58**, 429 (1973).
- [47] W. Bartel et al., Phys. Lett. B **39**, 407 (1972).
- [48] J. Bermuth et al., Phys. Lett. B **564**, 199 (2003).
- [49] G. Kubon et al., Phys. Lett. B **524**, 26 (2002).
- [50] R. Madey et al. (E93-038), Phys. Rev. Lett. **91**, 122002 (2003).
- [51] P. Markowitz et al., Phys. Rev. C **48**, R5 (1993).
- [52] B. Plaster et al. (Jefferson Laboratory E93-038), Phys. Rev. C **73**, 025205 (2006).
- [53] D. Rohe et al., Phys. Rev. Lett. **83**, 4257 (1999).
- [54] B. Bhattacharya et al., Phys. Rev. D **84**, 073006 (2011).